J|A|C|S ARTICLES

Published on Web 03/23/2009

Electrostatic Control of the Photoisomerization Efficiency and Optical Properties in Visual Pigments: On the Role of Counterion Quenching

Gaia Tomasello,[†] Gloria Olaso-González,[‡] Piero Altoè,[†] Marco Stenta,[†] Luis Serrano-Andrés,[‡] Manuela Merchán,*[,‡] Giorgio Orlandi,[†] Andrea Bottoni,[†] and Marco Garavelli*[,†]

Dipartimento di Chimica "G. Ciamician", Università di Bologna, via Selmi 2, Bologna I-40126, Italy, and Instituto de Ciencia Molecular, Universitat de València, ES-46071 Valencia, Spain

Received October 28, 2008; E-mail: Manuela.Merchan@uv.es; marco.garavelli@unibo.it

Abstract: Hybrid QM(CASPT2//CASSCF/6−31G*)/MM(Amber) computations have been used to map the photoisomerization path of the retinal chromophore in Rhodopsin and explore the reasons behind the photoactivity efficiency and spectral control in the visual pigments. It is shown that while the electrostatic environment plays a central role in properly tuning the optical properties of the chromophore, it is also critical in biasing the ultrafast photochemical event: it controls the slope of the photoisomerization channel as well as the accessibility of the S_1/S_0 crossing space triggering the ultrafast decay. The roles of the E113 counterion, the E181 residue, and the other amino acids of the protein pocket are explicitly analyzed: it appears that counterion quenching by the protein environment plays a key role in setting up the chromophore's optical properties and its photochemical efficiency. A unified scenario is presented that discloses the relationship between spectroscopic and mechanistic properties in rhodopsins and allows us to draw a solid mechanism for spectral tuning in color vision pigments: a tunable counterion shielding appears as the elective mechanism for L↔M spectral modulation, while a retinal conformational control must dictate S absorption. Finally, it is suggested that this model may contribute to shed new light into mutations-related vision deficiencies that opens innovative perspectives for experimental biomolecular investigations in this field.

1. Introduction

The protonated Schiff base of the 11-*cis* retinal (PSB11) is the chromophore of visual pigments.[1−6] These include rhodopsin (Rh) that peaks at 498 nm[7] and is used in twilight vision and the human three color vision pigments that peak at 425 nm (S-cone or blue), 530 (M-cone or green), and 560 nm (L-cone or red).[7,8] The biological activity of rhodopsins is triggered by the ultrafast (200 fs in Rh, see eq 1) light-induced *cis*−*trans* isomerization of the corresponding retinal chromophores that, in turn, induces a conformational change in the protein on longer time scales.[1,5] This ultrashort photochemical step is usually referred to as the primary event of the protein photocycle.

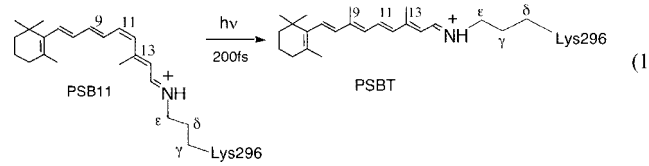

(1)

We have previously reported[9−14] the results of *ab initio* CASPT2//CASSCF minimum energy path (MEP) mapping for the photoisomerization *in vacuo* of reduced models of the retinal

[†] Università di Bologna.
[‡] Universitat de València.

(1) Kandori, H.; Shichida, Y.; Yoshizawa, T. *Biochemistry (Moscow)* **2001**, *66*, 1197.
(2) Needleman, R. Bacteriorhodopsin and Rhodopsin. In *CRC Handbook of Organic Photochemistry and Photobiology*; Horspool, W. M., Song, P.-S., Eds.; CRC Press: Boca Raton, FL, 1995; pp 1508−1515.
(3) Ottolenghi, M.; Sheves, M. *Isr. J. Chem.* **1995**, *35*, U3.
(4) Wald, G. *Science* **1968**, *162*, 230.
(5) Mathies, R.; Lugtenburg, J. The Primary Photoreaction of Rhodopsin. In *Molecular Mechanism of Vision*; Stavenga, D. G., DeGrip, W. J., Pugh, E. N. J., Eds.; Elsevier Science Press: New York, 2000; Vol. 3, pp 55−90.
(6) Yoshizawa, T.; Kuwata, O. Vision: Photochemistry. In *CRC Handbook of Organic Photochemistry and Photobiology*; Horspool, W. M., Song, P.-S., Eds.; CRC Press: Boca Raton, FL, 1995; pp 1493−1499.
(7) Wald, G.; Brown, P. K. *Science* **1958**, *127*, 222.
(8) McBee, J. K.; Palczewski, K.; Baehr, W.; Pepperberg, D. R. Confronting Complexity: The Interlink of Phototransduction and Retinoid Metabolism in Vertebrate Retina. In *Progress in Retinal and Eye Research*; Osborn, N. N., Chader, G. J., Eds.; Elsevier: U.K., 2001; Vol. 20, p 469.
(9) Garavelli, M.; Bernardi, F.; Olivucci, M.; Vreven, T.; Klein, S.; Celani, P.; Robb, M. A. *Faraday Discuss.* **1998**, *110*, 51.
(10) González-Luque, R.; Garavelli, M.; Bernardi, F.; Merchán, M.; Robb, M. A.; Olivucci, M. *Proc. Natl. Acad. Sci. U.S.A.* **2000**, *97*, 9379.
(11) Cembran, A.; Bernardi, F.; Olivucci, M.; Garavelli, M. *J. Am. Chem. Soc.* **2003**, *125*, 12509.
(12) De Vico, L.; Page, C. S.; Garavelli, M.; Bernardi, F.; Basosi, R.; Olivucci, M. *J. Am. Chem. Soc.* **2002**, *124*, 4124.
(13) Garavelli, M.; Vreven, T.; Celani, P.; Bernardi, F.; Robb, M. A.; Olivucci, M. *J. Am. Chem. Soc.* **1998**, *120*, 1285.
(14) Garavelli, M.; Celani, P.; Bernardi, F.; Robb, M. A.; Olivucci, M. *J. Am. Chem. Soc.* **1997**, *119*, 6891.

 10.1021/ja808424b CCC: $40.75

chromophore, and very recently, the results for the real (i.e., unreduced) PSB11 chromophore have been presented.[15] It has been shown that the reaction mechanism is characterized by a *two-mode* photoisomerization path (first stretching then one-bond-flip (OBF)[16,17] torsion of the reacting double bond) that develops entirely on the spectroscopic (charge transfer) state S_1. This path is essentially barrierless and drives the system into a central double bond twisted S_1/S_0 conical intersection (CI) funnel whose geometry and electronic structure are consistent with those of a twisted intramolecular charge transfer (TICT) state.[10,12,13] This point triggers the ultrafast decay to the ground state and prompts an efficient photoproduct formation.

While the aforementioned results disclose the intrinsic photoisomerization ability of the retinal chromophore, environmental factors (such as the ones involved in the solvent or protein) are known to affect both its spectroscopy and photochemistry.[18] For instance, the absorption maximum in Rh, 498 nm, appears to be red-shifted with respect to the one observed in solution (440 nm), and the protein structure itself plays a role in the spectral tuning of the pigments as revealed by the three (S, M, and L) color vision pigments (in this context, the spectral effects of the substitution of one or more amino acids have been widely investigated experimentally).[8,19,20] Second, while in the protein the photoreaction is finalized in 200 fs with a high (ca. 67%) quantum yield (QY)[21,22] under stereoselective control (i.e., only the *all-trans* (PSBT) photoproduct is produced), the isolated chromophore in solution (e.g., methanol or hexane) features a biexponential excited-state decay dynamics with a dominant (almost 20-fold longer) 2 ps component,[21,23,24] the stereoselectivity is lost, and the QY decreases (ca. 25%).[21,25] Consistently, an excited-state energy barrier has been observed for PSBT in solvent,[23] while no barriers are expected for Rh due to the subpicosecond nature of the process,[9,11] arising questions on the origin of the protein catalytic effect that makes this event one of the fastest photochemical reactions observed so far in nature.

It is apparent that both steric and electrostatic interactions between the chromophore and the surrounding protein pocket must play a key role in tuning/controlling the photochemical and photophysical behavior of the system. The reasons behind the optical properties and catalytic effect of Rh have been widely investigated in the past both experimentally and computationally. Those works reveal that different cooperative effects are responsible for the increased efficiency and photoisomerization rate observed in the visual pigment. For instance, previous experimental works by Mathies and co-workers[26] have shown that intramolecular steric interactions between the retinal C_{10}-hydrogen and the C_{13}-methyl do significantly affect the efficiency (i.e., QY and rate) of the photoisomerization process. Consistently with this view, Buss and co-workers[27] have recently shown that the ground-state twists of the C_{11}═C_{12} and the C_{12}—C_{13} bonds (which are mainly due to interaction with the Rh protein pocket) help to effectively and rapidly transfer stretch energy into torsion energy and thus populate efficiently the isomerization coordinate. Furthermore, recent reports on crystal structures of Rh[28,29] have pointed out the close proximity of Cys-187 with the retinal C_{12}-hydrogen, suggesting how such an interaction could lead to enhanced isomerization upon photoexcitation. Besides steric interactions, also electrostatic effects are expected to play a major role in photoisomerization catalysis as the photoactive state S_1 has a charge transfer nature and its energy is expected to depend on interactions with surrounding charged residues and polar groups. The same holds (for the same reasoning) for the TICT S_1/S_0 CI funnel and, more generally, for the S_1/S_0 crossing seam. In fact, its position is dictated by external charges that may displace the S_1/S_0 crossing seam out of the ideal photoisomerization channel or can even remove it.[18,30] Anyway, while steric effects on the photoisomerization have been deeply analyzed, studies on electrostatic effects appear to be mainly focused on static spectral properties (i.e., vertical excitations) rather than on the efficiency of the photochemical reaction, and to the best of our knowledge no precise and systematic analysis of these effects on the photoisomerization ability of the chromophore in the visual pigments is available to date. For example, a static as well as dynamical molecular level description of the primary photoisomerization event in Rh has been recently reported by Olivucci and co-workers[31−33] using Quantum Mechanics/Molecular Mechanics (QM/MM)[34] computations at the multiconfigurational (CASSCF)/correlated energy (CASPT2) resolution. This is the reference simulation to date on Rh photoreaction. Nevertheless, the study does not focus on or analyze the reasons behind Rh photoisomerization efficiency, such as environment electrostatic effects. Among these, the interaction with the formal E113 counterion and nearby charged/polar residues must be carefully analyzed as they are likely to be the principal contributors of these effects. Interestingly, the protonation state of the E181 residue (that is located right above the photoactive central double bond of the chromophore)[28,29,35] has been recently reconsidered: while previous two-photon absorption[36] and mutation experiments[37,38] seemed to

(15) Cembran, A.; González-Luque, R.; Serrano-Andrés, L.; Merchán, M.; Garavelli, M. *Theor. Chem. Acc.* **2007**, *118*, 173.
(16) Turro, N. J. *Modern Molecular Photochemistry*; Benjamin-Cummings: Menlo Park, CA, 1991.
(17) Gilbert, A.; Baggott, J. *Essentials of Molecular Photochemistry*; Blackwell Science: Oxford, 1991.
(18) Cembran, A.; Bernardi, F.; Olivucci, M.; Garavelli, M. *J. Am. Chem. Soc.* **2004**, *126*, 16018.
(19) Nathans, J.; Piantanida, T. P.; Eddy, R. L.; Shows, T. B.; Hogness, D. S. *Science* **1986**, *232*, 203.
(20) Kochendoerfer, G. G.; Lin, S. W.; Sakmar, T. P.; Mathies, R. A. *Trends Biochem. Sci.* **1999**, *24*, 300.
(21) Hamm, P.; Zurek, M.; Roschinger, T.; Patzelt, H.; Oesterhelt, D.; Zinth, W. *Chem. Phys. Lett.* **1996**, *263*, 613.
(22) Kandori, H.; Sasabe, H.; Nakanishi, K.; Yoshizawa, T.; Mizukami, T.; Shichida, Y. *J. Am. Chem. Soc.* **1996**, *118*, 1002.
(23) Logunov, S. L.; Song, L.; ElSayed, M. A. *J. Phys. Chem.* **1996**, *100*, 18586.
(24) Kandori, H.; Katsuta, Y.; Ito, M.; Sasabe, H. *J. Am. Chem. Soc.* **1995**, *117*, 2669.
(25) Freedman, K. A.; Becker, R. S. *J. Am. Chem. Soc.* **1986**, *108*, 1245.
(26) Kochendoerfer, G. G.; Verdegem, P. J. E.; vanderHoef, I.; Lugtenburg, J.; Mathies, R. A. *Biochemistry* **1996**, *35*, 16230.
(27) Sugihara, M.; Hufen, J.; Buss, V. *Biochemistry* **2006**, *45*, 801.
(28) Teller, D. C.; Okada, T.; Behnke, C. A.; Palczewski, K.; Stenkamp, R. E. *Biochemistry* **2001**, *40*, 7761.
(29) Okada, T.; Sugihara, M.; Bondar, A. N.; Elstner, M.; Buss, V. *J. Mol. Biol.* **2004**, *342*, 571.
(30) Cembran, A.; Bernardi, F.; Olivucci, M.; Garavelli, M. *Proc. Natl. Acad. Sci. U.S.A.* **2005**, *102*, 6255.
(31) Andruniów, T.; Ferré, N.; Olivucci, M. *Proc. Natl. Acad. Sci. U.S.A.* **2004**, *101*, 17908.
(32) Migani, A.; Sinicropi, A.; Ferre, N.; Cembran, A.; Garavelli, M.; Olivucci, M. *Faraday Discuss.* **2004**, *127*, 179.
(33) Frutos, L. M.; Andruniow, T.; Santoro, F.; Ferre, N.; Olivucci, M. *Proc. Natl. Acad. Sci. U.S.A.* **2007**, *104*, 7764.
(34) Lin, H.; Truhlar, D. G. *Theor. Chem. Acc.* **2006**, *117*, 185.
(35) Palczewski, K.; Kumasaka, T.; Hori, T.; Behnke, C. A.; Motoshima, H.; Fox, B. A.; Le Trong, I.; Teller, D. C.; Okada, T.; Stenkamp, R. E.; Yamamoto, M.; Miyano, M. *Science* **2000**, *289*, 739.
(36) Birge, R. R.; Murray, P. P.; Pierce, B. M.; Akita, H.; Balogh-Nair, V.; Findsen, L. A.; Nakanishi, K. *Proc. Natl. Acad. Sci. U.S.A.* **1985**, *82*, 4117.

suggest a neutral binding site and assigned it to a neutral (i.e., protonated) species, recent experimental[39−41] and computational studies[42] suggest a deprotonated (i.e., negatively charged) 181 residue. Implications of this nearby negative charge on the photoisomerization efficiency and stereoselectivity have been suggested.[18,30,41] Among others, these still unresolved issues represent a stimulus for the present QM/MM investigation, although here a more systematic study of all (both close and far) residues playing a role on these effects is considered.

As mentioned above, Rh absorption peaks at 498 nm.[7] This is a well established result, whereas uncertainties exist for the absorption values of higher energy states. The Rh absorption spectrum recorded by Ebrey and Honig[43] displays, in addition to the dominant 498 nm component, a second smaller maximum at a shorter wavelength peaking at ∼340 nm. This should refer to a less absorbing higher energy state with an oscillator strength that is roughly one-third of S_1, as the inspection of the spectrum approximately reveals. Two-photon absorption experiments by Birge and co-workers[36] on Rh (containing a 11-cis-locked retinal analogue to prevent bleaching) suggest an S_2 (covalent dark A_g-like) state that is only 2000 cm^{-1} above S_1 (which would lead to a vertical 63 kcal/mol (i.e., 453 nm) energy value for this state). If this were the case, the higher energy 340 nm band observed by Ebrey and Honig would originate from a state higher than S_2. Anyway, based on the absorption values recorded for isolated retinal chromophores in the gas phase (that place the signatures of the S_2 state at much higher energies), Andersen and co-workers[44] have very recently reassigned the observed 2000 cm^{-1} two-photon absorption band to a vibrational feature of the bright lowest energy S_1 state spectrum, thus suggesting that S_2 does correspond indeed to the 340 nm band.

In recent computational investigations, both Buss[45] and Olivucci[31] successfully reproduced Rh absorption by applying the same approach (with the former value in remarkable good agreement with the experimental data): multireference perturbation level (CASSCF(12,12)/CASPT2) calculations on the chromophore put in the bath of the protein point charges. Anyway, the protein embedded retinal structure employed to compute spectroscopic properties was optimized according to a DFT-based and CASSCF method, respectively. Interestingly, the reasons leading to reproduction of the correct absorption value are contrasting and striking differences in the two cases. In the former, the Rh electrostatic environment is shown to have only a very minor effect on the absorption properties of the chromophore/counterion (E113) couple (that alone does almost reproduce the correct S_1 energy found in the protein), while in the latter this effect is major as it quenches (i.e., counterbalance) almost fully the electrostatic effect of the counterion, basically recovering the absorption energy computed for the isolated distorted (i.e., optimized within the protein) chromophore (that alone does already almost reproduce the value observed in the protein). Additionally, Buss reproduces fairly well (66.7 kcal/mol)[45] the lower energy value reported by Birge for S_2 (63 kcal/mol),[36] while for the same (i.e., covalent A_g-like) S_2 state Olivucci replicates satisfactorily (87.5 kcal/mol)[31] the 340 nm (84 kcal/mol) absorption feature observed by Ebrey and Honig.[43] While those results were both obtained considering a neutral Glu-181 residue, more recently Bravaya et al. (yet applying another perturbative QM/MM approach) successfully reproduced Rh absorption (as well as the gas and solution values)[46] using a charged E181; shielding of the counterion by the protein field was also predicted in this case. Additionally, recent SAC-CI QM/MM computations[47] also nicely predicted S_1 excitation (using a neutral E181), but no shielding emerged. Finally, Altun et al.[48] have very recently reproduced Rh absorption as well (and that of its mutants) employing a DFT/TD-DFT QM/MM procedure: E181 was still considered neutral, and the counterion was predicted to produce a much smaller blue shift (from 4 to 6 kcal/mol only) than in all previous studies and to be unquenched by the protein (i.e., the net effect of the other amino acids is negligible). It is apparent that all those contrasting findings call for a major reinvestigation of Rh spectroscopic properties. This is far from being just a simple academic issue, as it involves disclosure of the role played by protein electrostatic effects in spectral tuning.

In this paper, the primary photochemical event of Rh and the singlet manifold characterizing this process are explored by *ab initio* multiconfigurational perturbation theory calculations (CASPT2//CASSCF) via adopting a novel (recently developed by our group) hybrid QM/MM procedure accounting for electrostatic embedding at the QM level.[49] The most recent and best-resolved crystallographic structure available for Rh is employed,[29] and the protein embedded photoisomerization path is mapped. While the structure of the photoisomerization coordinate in Rh is not the focus of this study (as it has been documented and discussed in detail elsewhere),[31−33] herein we provide information on the effects that the protein electrostatic environment may exercise on the (i) optical (i.e., spectral tuning) and (ii) photoreactivity properties of rhodopsins. For this purpose, the effect of both close and distant residues is explicitly accounted for and analyzed. While we do not want to reject or question other effects that have been previously recognized in photoisomerization catalysis, here we provide computational evidence for a mechanism of electrostatic control in the photoactivity of visual pigments that have not been recognized before. A thoughtful discussion of all the most recent experimental/computational findings compared to the presented results is shown, which supports this new view. Finally, a unified model

(37) Yan, E. C. Y.; Kazmi, M. A.; De, S.; Chang, B. S. W.; Seibert, C.; Marin, E. P.; Mathies, R. A.; Sakmar, T. P. *Biochemistry* **2002**, *41*, 3620.
(38) Yan, E. C. Y.; Kazmi, M. A.; Ganim, Z.; Hou, J. M.; Pan, D. H.; Chang, B. S. W.; Sakmar, T. P.; Mathies, R. A. *Proc. Natl. Acad. Sci. U.S.A.* **2003**, *100*, 9262.
(39) Lewis, J. W.; Szundi, I.; Kazmi, M. A.; Sakmar, T. P.; Kliger, D. S. *Biochemistry* **2004**, *43*, 12614.
(40) Terakita, A.; Yamashita, T.; Shichida, Y. *Proc. Natl. Acad. Sci. U.S.A.* **2000**, *97*, 14263.
(41) Ludeke, S.; Beck, R.; Yan, E. C. Y.; Sakmar, T. P.; Siebert, F.; Vogel, R. *J. Mol. Biol.* **2005**, *353*, 345.
(42) Rohrig, U. F.; Guidoni, L.; Rothlisberger, U. *Biophys. J.* **2002**, *82*, 223A.
(43) Ebrey, T. G.; Honig, B. *Proc. Natl. Acad. Sci. U.S.A.* **1972**, *69*, 1897.
(44) Nielsen, I. B.; Lammich, L.; Andersen, L. H. *Phys. Rev. Lett.* **2006**, *96*, 018304. Although this work refers to bR 2-photon spectra, a parallel reasoning holds for Rh too, due to the similarity of the two spectra: Rh and bR give very similar outcomes in two-photon experiments; namely a very low energy S_2 signature (very close to S_1) has been assigned both in Rh and bR in the 2-photon experiments, which has been questioned by Andersen and coworkers. In conclusion, the assignment of the S_2 feature in Rh is still far from being unbiased and fully solved.
(45) Sekharan, S.; Sugihara, M.; Buss, V. *Angew. Chem., Int. Ed.* **2007**, *46*, 269.
(46) Bravaya, K.; Bochenkova, A.; Granovsky, A.; Nemulkhin, A. *J. Am. Chem. Soc.* **2007**, *129*, 13035.
(47) Fujimoto, K.; Hayashi, S.; Hasegawa, J.; Nakatsuji, H. *J. Chem. Theory Comput.* **2007**, *3*, 605.
(48) Altun, A.; Yokoyama, S.; Morokuma, K. *J. Phys. Chem. B* **2008**, *112*, 6814.
(49) Altoè, P.; Stenta, M.; Bottoni, A.; Garavelli, M. *Theor. Chem. Acc.* **2007**, *118*, 219.

is drawn that discloses the relationship between spectroscopic and mechanistic properties in Rh and related (blue, green, and red) color vision pigments. This leads to formulating a solid mechanism for spectral tuning in color vision pigments. It is anticipated here that these findings may open novel scenarios in the rationale of mutations-dependent vision deficiencies.

2. Computational Details

All computations are performed using a new hybrid QM/MM[34] potential recently developed by our group.[49] Details of this hybrid approach are presented elsewhere (see also the Supporting Information). Briefly, the method is based on a hydrogen link-atom scheme.[50] QM and MM layers interact in the following way: (i) all QM atoms feel the electrostatic potential of all MM point charges (i.e., an electrostatic embedding scheme has been adopted); (ii) all the bonding (i.e., stretching, bending, and torsion) and the Van der Waals QM/MM cross terms are described by the standard MM potential; and (iii) electrostatic interactions involving MM atoms are all accounted for classically. In this case, the QM−MM frontier is placed at the $C_\delta-C_\epsilon$ bond of the Lys-296 side chain (see eq 1). The QM region (i.e., the chromophore atoms) is treated by ab initio CASSCF/6−31G* computations using the Gaussian03[51] suite of programs (a complete active space of 12 π-electrons in 12 π-orbitals (12e/12o) is employed to describe the CASSCF wave function), while the AMBER8[52] software and the *ff99* force field[52] is used for the MM region (i.e., the opsin) and its charges. CASSCF/AMBER QM/MM computations are accomplished using the COBRAMM interface,[49] implemented by our group, that links Gaussian03[51] and AMBER8[52] packages.

Protein chain (the monomer A) of the recently crystallized and best-resolved X-ray structure available for bovine Rh (PDB code: 1U19, resolution = 2.2 Å),[29] which has no missing amino acids, is used for the protein framework. Hydrogen atoms are added by means of the H++ software.[53] In general, all titratable groups are carefully reconsidered, and through an accurate analysis the following choice is adopted: the Glu-113 counterion is taken charged, Glu-122 is neutral, Glu-181 is considered both charged and neutral in two different protein setups ($Rh_{181(-)}$ and Rh_{181H}, respectively), all other glutamate residues are charged, lysine residues are protonated, Asp-83 is protonated, and three (Hip-65, Hip-100, Hip-278) of the six hystidine residues are protonated.

The protein framework is kept fixed during all QM/MM geometry optimizations (we assumed that it has no time to change during the ultrafast (200 fs) time scale of the primary photoinduced event), while all QM atoms and MM atoms comprising the Lys-296 side chain ($C_\delta H_2$, $C_\gamma H_2$, $C_\beta H_2$) and the two water molecules (W1 and W2, that are described by TIP3P) are left free to relax.

An S_0-S_n *n*-root state average CASSCF wave function (equally weighting all the *n* roots) is always used for geometry optimizations on the S_n state, while a single-state wave function is used for ground-state optimizations. A relaxed scan (with the central dihedral angle fixed at specified values) is used to trace the photoisomerization channel in the protein, while fully unconstrained optimizations are employed to locate all the critical points.

To account for correlation energy, both CASPT2[54] and MS-CASPT2[55,56] single-point computations are performed on the optimized points in the bath of the protein (AMBER) point charges, by using the MOLCAS-6.0 package.[57] Unless otherwise stated, a three-root state average wave function is employed. To minimize the influence of weakly interacting intruder states at the second-order level, the so-called imaginary level shift technique is used (imaginary shift value = 0.2).[10] QM(CASPT2)/MM energies are taken as the reference values throughout the work, while MS-CASPT2 corrections are considered only when a multistate problem appears (this happens only in one specific situation as will be discussed in the text below); see also Supporting Information for details. The CASSCF state interaction (CASSI) method[58] is used (as implemented in MOLCAS-6.0[57]) to calculate the transition dipole moments. Oscillator strengths (*f*) are computed using CASSCF transition moments and CASPT2 corrected energies.

The charge distribution along the chromophore chain is evaluated according to state-averaged CASSCF wave functions by Mulliken charge analysis and is used to characterize the electronic nature (i.e., ionic vs covalent) of the investigated states.

A Reverse Fingerprint (RFP) analysis is employed on the investigated residues to highlight their electrostatic effects on the excitation energy: this is done by switching off specifically the charges of the investigated residue (while leaving on all the other charges of the protein environment) and recording the CASPT2 (blue or red) shift in the chromophore S_1 excitation energy with respect to the reference Rh value (that is represented by the zero line in the corresponding figure; see below).

Table 1. CASPT2 Relative Energies (ΔE, kcal/mol) for the Lowest Three Singlet States of Two Different Protein Setups ($Rh_{181(-)}$ and Rh_{181H})[a]

protein structure	chromophore state (electronic nature)	ΔE	$f_{S_0\rightarrow S_n}$	wavefunction[b] (coefficient)
$Rh_{181(-)}$	S_0 (A_g-like)	0.0	0.00	$(6a)^2\ (7a)^0$ (0.77)
	S_1 (B_u-like)	57.6	0.74	$(6a)^1\ (7a)^1$ (0.63)
	S_2 (A_g-like)	82.0	0.27	$(6a)^0\ (7a)^2$ (0.11)
				$(6a)^1\ (7a)^1$ (0.19)
Rh_{181H}	S_0 (A_g-like)	0.0	0.00	$(6a)^2\ (7a)^0$ (0.77)
	S_1 (B_u-like)	53.6	0.75	$(6a)^1\ (7a)^1$ (0.64)
	S_2 (A_g-like)	81.6	0.28	$(6a)^0\ (7a)^2$ (0.10)
				$(6a)^1\ (7a)^1$ (0.18)

[a] Oscillator strengths for ground state excitations ($f_{S_0\rightarrow S_n}$) and wavefunction characterization are also reported. [b] 6a and 7a represent the HOMO and LUMO π orbitals, respectively.

3. Results and Discussion

3.1. The Glu181 Issue: Neutral or Protonated. Inspired by the recent works[39−42] that have readdressed the charge state of the Glu-181 residue in Rh (considered neutral so far), the chromophore structure has been optimized into both a neutral (Rh_{181H}) and negatively charged ($Rh_{181(-)}$) protein binding pocket, corresponding to a neutral (i.e., protonated) or a charged (i.e., deprotonated) Glu-181 residue, respectively. Table 1 reports CASPT2 vertical energies computed for the S_1 (ionic/charge-transfer B_u-like) and S_2 (covalent A_g-like) states of the chromophore optimized in the ground state of the two different setups together with their oscillator strengths and wave function characterization. Interestingly, while Rh_{181H} leads to an S_1 energy (53.6 kcal/mol) that is slightly underestimated with respect to the observed absorption value (peaking at 57.4 kcal/mol, i.e. 498 nm), $Rh_{181(-)}$ reproduces remarkably well this energy (57.6 kcal/mol). On the other hand, S_2 appears unaffected by the

(50) Singh, U. C.; Kollman, P. A. *J. Comput. Chem.* **1986**, *7*, 718.
(51) Frisch, M. J. *Gaussian 03*, revision C.02; Gaussian, Inc.: Wallingford, CT, 2004.
(52) Case, D. A.; Cheatham, T. E.; Darden, T.; Gohlke, H.; Luo, R.; Merz, K. M.; Onufriev, A.; Simmerling, C.; Wang, B.; Woods, R. J. *J. Comput. Chem.* **2005**, *26*, 1668.
(53) Gordon, J. C.; Myers, J. B.; Folta, T.; Shoja, V.; Heath, L. S.; Onufriev, A. *Nucleic Acids Res.* **2005**, *33*, 368.
(54) Andersson, K.; Malmqvist, P. A.; Roos, B. O. *J. Chem. Phys.* **1992**, *96*, 1218.
(55) Malmqvist, P. A.; Roos, B. O.; Serrano-Andres, L. *Chem. Phys. Lett.* **1998**, *288*, 299.
(56) Serrano-Andres, L.; Merchán, M.; Lindh, R. *J. Chem. Phys.* **2005**, *122*, 104107.
(57) Andersson, K. *MOLCAS*, 6.0; Department of Theoretical Chemistry, Chemical Centre, University of Lund: Lund, 2004.
(58) Malmqvist, P.-Å.; Roos, B. O. *Chem. Phys. Lett.* **1989**, *155*, 189.

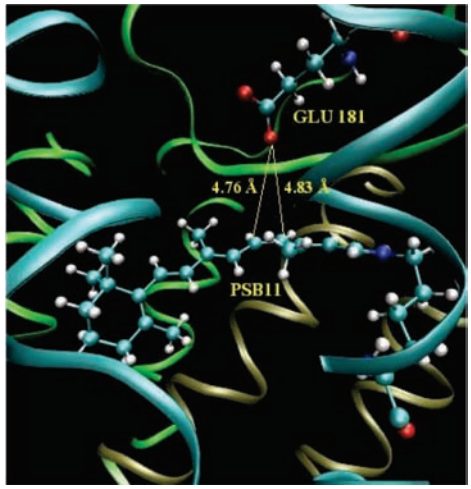

Figure 1. Retinal binding pocket in Rh drawn from its crystallographic structure.[29] It is apparent that Glu-181 is placed right above the central C_{11}=C_{12} double bond of the chromophore, in a symmetric position with respect to its β-ionone tail and protonated Schiff base head.

electrostatic environment, leading to an energy value that is ca. 82 kcal/mol in both cases. This is consistent with S_2 possessing the same electronic nature as S_0 (covalent A_g-like; i.e., they have a similar electronic density distribution), leading to an S_0-S_2 energy gap that is barely affected by external electrostatic effects. This value and its computed oscillator strength (0.3, see Table 1) nicely agree with the secondary (less intense) higher energy absorption feature observed in Rh at 340 nm (84 kcal/mol) by Ebrey and Honig.[43] Note also that it greatly differs from the other experimental value (by two-photon absorption) observed by Birge and co-workers[36] that is much closer to the value computed by Buss.[45] Nonetheless, the covalent S_2 state assignment from two-photon experiments has been recently questioned[44] so that uncertainties still exist on the S_2 absorption energy in rhodopsin-type proteins. It is worth noting that this may be very valuable information since it would provide an outstanding test for QM/MM approaches, as it appears that very different energies are predicted for this state in Rh according to the different computational approaches employed.

Although this spectroscopic scenario is in qualitative agreement with the one reported by Olivucci and co-workers, [31] the quantitative agreement with the experiments appear to be significantly improved. Furthermore, an electrostatic environment (with a charged Glu-181) that is different than the one conventionally used has been considered here (as also done in a recent work by Bravaya et al.[46]).

While a charged Glu-181 residue is consistent with the changes observed in the spectrum of some 181-mutated Rh (e.g., E181Q and E181D),[39] it is in contrast with other mutations[37,38] that revealed a very minor effect on the S_1 absorption energy due to 181 substitution and that were taken as a proof for a neutral Glu-181. It is apparent that absorbance measurements on Rh mutants do not give a clear-cut answer about whether E181 is ionized in the dark. This is not surprising as this residue is placed right above the central C_{11}=C_{12} double bond of retinal (i.e., in a symmetric position with respect to the PSB head and the β-ionone tail of the chromohore that supports charge translocation upon photoexcitation to S_1; see Figure 1), which makes S_1 rather insensitive to its protonation state, as recent computational investigations indeed reveal.[18,30,46] This has also been pointed out recently by Kliger and co-workers.[39] Consistently, it must be noted that the computed effect of Glu-181 ionization on S_1 absorption, although not negligible (ca. 3 kcal/mol), is very much less than the one expected in general for a nearby charged residue (e.g., the effect of the Glu-113 counterion residue (ca. 0.6 eV) reported and discussed below). As its protonation state has much less impact on Rh absorbance than generally assumed, mutation experiments must be carefully analyzed. A number of other experimental/computational evidence have been very recently collected that suggest a charged Glu-181, specifically: (i) Glu-181 acts as the counterion in invertebrate rhodopsins;[40,59] (ii) Glu-181 must be ionized to stabilize the late photointermediates (e.g., MI) and make efficient the photoactivation cycle of visual pigments (the so-called Glu-113/Glu-181 *counterion switch model*);[37,38,60,61] (iii) Glu-181 is deprotonated (together with the primary counterion) in the mouse short-wavelength sensitive visual pigment (MUV);[60,61] (iv) Glu-181 is the counterion in parapinopsin that shares with Rh a great sequence identity;[59] (v) FTIR spectroscopy studies[41] and MD simulations[42] of Rh are consistent with a negatively charged Glu-181 in the ground state. Taken all together and jointly with the present results, these findings suggest a deprotonated 181 residue and an overall negatively charged binding pocket.

To disclose the possible effects that the protonation state of Glu-181 may have on the chromophore photoisomerization ability, the photoisomerization channel is computed for both Rh_{181H} and $Rh_{181(-)}$, and the two paths are reported and compared in Figure 2. Since Glu-181 is positioned near the center of the chromophore, no significant effects are foreseen on the photoisomerization process for the same reasons discussed above. Consistently, Figure 2 shows that the photoreaction efficiency is the same regardless of its protonation state: both the slope and the CI funnel are unaffected. These results seem to question the possible involvement of the Glu-181 residue in assisting the primary photochemical event, invoking its role "only" in the stabilization of the later photocycle intermediates and the promotion of Rh photoactivation (as according to the counterion switch model).[37,38,60,61] In this respect, and according to the presented results, both Rh_{181H} and $Rh_{181(-)}$ can be safely utilized to properly study the primary photoisomerization event and its mechanism. Additionally, it must be said that our results cannot be considered as conclusive proof for the Glu-181 protonation state, as the accuracy of the methodology is not sufficient to make a certain statement. The intrinsic accuracy of CASPT2 is on the order of 0.1 eV, and the basis set used may have some impact as well. The point charge approximation used to simulate the protein electrostatic force field (including the counterion effect) and the lack of protein polarizability may be further sources of approximation. A more focused computational analysis involving different approaches and tools, such as protein relaxation and dynamics, would be better suited to disclose this issue. Anyway, since $Rh_{181(-)}$ does reproduce remarkably well the spectroscopic properties observed in Rh, it agrees with some of the most recent experimental findings on this topic (as discussed above), and since the results presented in this paper are unaffected by the protonation state of Glu-181, we will consider this setup thereafter for Rh.

(59) Terakita, A.; Koyanagi, M.; Tsukamoto, H.; Yamashita, T.; Miyata, T.; Shichida, Y. *Nat. Struct. Mol. Biol.* **2004**, *11*, 284.
(60) Kusnetzow, A. K.; Dukkipati, A.; Babu, K. R.; Ramos, L.; Knox, B. E.; Birge, R. R. *Proc. Natl. Acad. Sci. U.S.A.* **2004**, *101*, 941.
(61) Ramos, L. S.; Chen, M. H.; Knox, B. E.; Birge, R. R. *Biochemistry* **2007**, *46*, 5330.

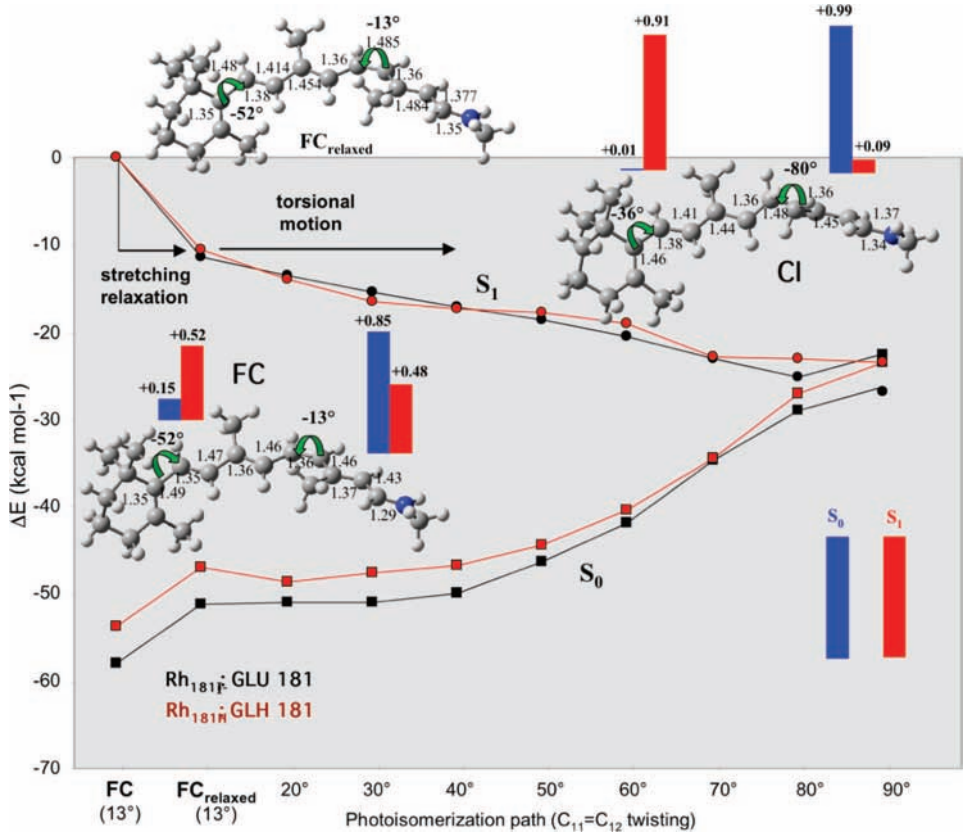

Figure 2. CASPT2 corrected S_0 and S_1 energy profiles along the QM(CASSCF)/MM relaxed scan on S_1 tracing the photoisomerization process in the two different Rh setups, from the Franck−Condon (FC) point to the twisted conical intersection funnel (CI), through a point ($FC_{relaxed}$) where only skeletal bond stretchings have been relaxed (i.e., dihedral angles have been frozen here). Bar diagrams display the fractional positive charge on each chromophore half with respect to the rotating central bond. Molecular parameters are reported in Å and degrees.

It is worth noting that previous QM/MM studies on Rh photoisomerization[31,33] surprisingly showed the existence of an intermediate (i.e., a minimum) on S_1 that seems apparently to contrast with the ultrafast photoisomerization observed in Rh. Although this fact does not appear to disfavor retinal subpicosecond photosiomerization dynamics (but this result is based on just a single MD simulation at 0 K),[33] in this work (starting from the best-resolved X-ray structure of Rh),[29] we partially revise this picture as we find a fully barrierless path with no excited-state intermediate and obtain a static description of the mechanism whose energies are more coherent with experimental observations. Obviously, the photoisomerization mechanism is the same as that documented before;[9,11] i.e., a complex reaction coordinate[29] is involved, differing from the simple OBF mode: that is, cooperative/concurrent twisting motions of adjacent C−C bonds result in a space saving mechanism that resembles (although aborted and developed only asynchronously and transiently) the bicycle pedal model proposed a few decades ago by Warshel in his pioneering computational studies[62,63] that already successfully predicted, by semiempirical molecular dynamics simulations, the correct 200 fs time scale for the photoisomerization process in Rh. Notably, the computed direction of twisting is in agreement with the sign of the initial C_{11}=C_{12} twist which has been previously derived[27,31,64] in Rh.

3.2. Counterion and the Other Polar/Charged Residues: Counterion Quenching by the Protein Pocket. In this section we will decompose the protein electrostatic effects eventually building up the absorption energy observed in Rh. This analysis appears to be relevant for spectral tuning but turns out to be crucial also for the photoisomerization efficiency, as it will be discussed further below.

3.2.1. Optical Properties. Table 2 shows how the S_1 (ionic, single excitation B_u-like) and S_2 (covalent, double excitation A_g-like) absorption properties change upon increasing the complexity of the system, i.e. from the isolated chromophore ($PSB11_{dist}$) to the full protein ($Rh_{181(-)}$), passing through the ion-pair ($PSB11_{dist}$−E113) system and shells of increasing size (i.e., comprising all the residues within a specified radius around the chromophore: $Rh_{r=2.0Å}$, $Rh_{r=2.2Å}$, $Rh_{r=2.5Å}$, $Rh_{r=3.0Å}$, $Rh_{r=3.5Å}$). Note that the chromophore structure is always the distorted one ($PSB11_{dist}$) optimized in the protein. This analysis allows us to progressively identify the protein residues that finally lead to the recorded Rh absorption. Scheme 1 summarizes these results graphically. As expected (see the discussion in the previous section), S_2 is much less affected by external charges and its energy remains substantially unchanged, while S_1 is very much sensitive to the electrostatic environment. Not surprisingly, the major effect on S_1 comes from the counterion (E113): an S_1 vertical absorption energy of 74.7 (CASPT2) and 65.7 (MS-CASPT2) kcal/mol is predicted in the $PSB11_{dist}$−E113 couple that is significantly blue-shifted (by ca. 25(CASPT2)/15(MS-CASPT2) kcal/mol) with respect to the value calculated in the bare chromophore $PSB11_{dist}$ (50.3 kcal/mol). The 15 kcal/mol (MS-CASPT2) blue shift effect is in quantitative agreement with

(62) Warshel, A. *Nature* **1976**, *260*, 679.
(63) Warshel, A. *Proc. Natl. Acad. Sci. U.S.A.* **1978**, *75*, 5250.
(64) Buss, V.; Kolster, K.; Terstegen, F.; Vahrenhorst, R. *Angew. Chem., Int. Ed.* **1998**, *37*, 1893.

Table 2. CASPT2 Relative Energies (ΔE, kcal/mol) for the Lowest Three Singlet States, Oscillator Strengths for Ground State Excitations ($f_{S_0 \rightarrow S_n}$) and Structure Characterization (List of Comprised Residues) for Systems of Increasing Size and Complexity[a]

structure	chromophore state (electronic nature)	ΔE	$f_{S_0 \rightarrow S_n}$	wave function[b] (coefficient)	residues
$PSB11_{dist}$	S_0	0.0	0.00	$(6a)^2$ $(7a)^0$ (0.78)	
	S_1	50.3	0.78	$(6a)^1$ $(7a)^1$ (0.65)	
	S_2	79.3	0.23	$(6a)^0$ $(7a)^2$ (0.15)	
				$(6a)^1$ $(7a)^1$ (0.13)	
$PSB11_{dist}$−E113	S_0	0.0[c] (0.0)	0.00	$(6a)^2$ $(7a)^0$ (0.75)	Glu-113
	S_1	65.7[c] (75.7)	0.86	$(6a)^1$ $(7a)^1$ (0.54)	
	S_2	95.2[c] (74.7)	0.11	$(6a)^0$ $(7a)^2$ (0.23)	
				$(6a)^1$ $(7a)^1$ (0.18)	
$Rh_{r=2.0Å}$	S_0	0.0	0.00	$(6a)^2$ $(7a)^0$ (0.75)	Glu-113, Ala-295, Lys-296, Thr-297
	S_1	67.2	0.62	$(6a)^1$ $(7a)^1$ (0.47)	
	S_2	77.4	0.35	$(6a)^0$ $(7a)^2$ (0.19)	
				$(6a)^1$ $(7a)^1$ (0.40)	
$Rh_{r=2.2Å}$	S_0	0.0	0.0	$(6a)^2$ $(7a)^0$ (0.75)	$Rh_{r=2.0Å}$ + Trp-265, Tyr-268, Met-207, Phe-212, Gly-121, Glh-122, Phe-293
	S_1	66.4	0.60	$(6a)^1$ $(7a)^1$ (0.49)	
	S_2	77.6	0.37	$(6a)^0$ $(7a)^2$ (0.20)	
				$(6a)^1$ $(7a)^{1\backslash}$ (0.39)	
$Rh_{r=2.5Å}$	S_0	0.0	0.00	$(6a)^2$ $(7a)^0$ (0.75)	$Rh_{r=2.2Å}$ + Phe-91, Gly-114, Cyx-187, Ile-189, Phe-261, Ala-292, Ser-298
	S_1	69.0	0.66	$(6a)^1$ $(7a)^1$ (0.49)	
	S_2	77.0	0.31	$(6a)^0$ $(7a)^2$ (0.20)	
				$(6a)^1$ $(7a)^1$ (0.39)	
$Rh_{r=3.0Å}$	S_0	0.0	0.00	$(6a)^2$ $(7a)^0$ (0.76)	$Rh_{r=2.5Å}$ + Ala-299, Met-44, Leu-47, Thr-94, Ala-117, Thr-118, Leu-125, Gly-188, Tyr-191, Phe-208, His-211, Phe-294
	S_1	62.2	0.43	$(6a)^1$ $(7a)^1$ (0.57)	
	S_2	79.6	0.46	$(6a)^0$ $(7a)^2$ (0.18)	
				$(6a)^1$ $(7a)^1$ (0.32)	
$Rh_{r=3.5Å}$	S_0	0.0	0.00	$(6a)^2$ $(7a)^0$ (0.76)	$Rh_{r=3.0Å}$ + Wat-358, Tyr-43, Tyr-178, Ser-186, Wat-354
	S_1	58.7	0.49	$(6a)^1$ $(7a)^1$ (0.61)	
	S_2	80.9	0.48	$(6a)^0$ $(7a)^2$ (0.17)	
				$(6a)^1$ $(7a)^1$ (0.27)	
Rh	S_0	0.0	0.00	$(6a)^2$ $(7a)^0$ (0.77)	full protein (all residues)
	S_1	57.6	0.74	$(6a)^1$ $(7a)^1$ (0.63)	
	S_2	82.0	0.27	$(6a)^0$ $(7a)^2$ (0.11)	
				$(6a)^1$ $(7a)^1$ (0.19)	

[a] The isolated chromophore ($PSB11_{dist}$), the ion pair ($PSB11_{dist}$−E113), protein shells of increasing size (i.e. comprising all the residues within a specified radius r around the chromophore: $Rh_{r=2.0Å}$, $Rh_{r=2.2Å}$, $Rh_{r=2.5Å}$, $Rh_{r=3.0Å}$, $Rh_{r=3.5Å}$), and the full protein (Rh). The chromophore structure is always the distorted one ($PSB11_{dist}$) optimized in the protein. [b] 6a and 7a represent the HOMO and LUMO π orbitals, respectively. [c] Multi-State CASPT2 results: S_1 and S_2 are degenerate at the CASPT2 level (values in brackets).

that calculated by Buss and co-workers[45] that is the computational reference on this topic up to now. Olivucci,[31] Bravaya,[46] and Nakatsuji[47] all predict a larger (>1 eV) value (which matches our CASPT2 value), while (quite surprisingly) DFT/TD-DFT ONIOM-based QM/MM computations on Rh very recently reported by Altun et al.[48] predict a much smaller blue shift effect (<0.5 eV) for the counterion that goes against all the other reported values.

Interestingly, CASPT2 and MS-CASPT2 energies are quite different in our case. In fact, while degeneration appears at CASPT2 for the ion pair between S_1 and S_2, this is removed after MS-CASPT2 corrections (see Table 2); i.e., a multistate problem emerges raising doubts on the real S_1/S_2 degeneracy and thus on the validity of the CASPT2 results. Indeed, we think that the MS-CASPT2 results are more accurate than the CASPT2 ones in this case. The arguments and the data supporting this statement are reported in detail in the Supporting Information. Here we just state that MS-CASPT2 replicates in general CASPT2 results for the structures investigated in this work (thus revealing that MS is a reliable approach in this case) but for the S_1/S_2 degenerate case occurring in the ion pair, where MS-CASPT2 returns energies that deviate significantly from the CASPT2 ones. Still, MS results are more reasonable: (i) they better fit literature data from other correlated methods,[46,47] as well as the results on the ion pair reported by Buss;[45] (ii) MS-CASPT2 S_1 Abs energy in the ion pair (430 nm) matches nicely the experimental energies for PSB11 in apolar solvent (440−460 nm) where analogous ion-pair systems should exist (on the other hand, standard CASPT2 results give an unrealistic much more blue-shifted value (380 nm, see Table 2) that has no experimental counterpart); (iii) a validation test has been performed at the ion pair by computing CASPT2 energies with an ANO type basis set (that is a better, although more expensive, choice than 6−31G* for (MS)CASPT2 computations), thus allowing a more accurate estimate of the correlation energy: remarkably, standard CASPT2/ANO-based computations return

Scheme 1

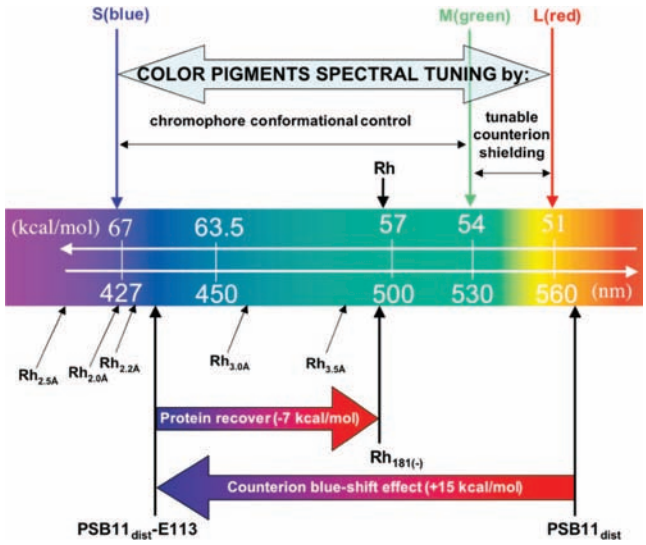

energies in agreement with the present MS/6−31G* results. This suggests that MS-CASPT2 should be the choice for the ion pair. Thus, we will consider the MS-CASPT2 values as the reference ones (i.e., the most accurate result) in this case, while standard CASPT2 results will be considered in all the other situations (see Computational Details and Supporting Information for a more in-depth discussion on this topic).

Interestingly, both the CASPT2 (74.7 kcal/mol) and MS-CASPT2 corrected (65.7 kcal/mol) values for S_1 in $PSB11_{dist}$−E113 (see Table 2) are far higher than the one simulated/observed in Rh (57.6/57.4 kcal/mol). It is apparent that a quenching by the protein of the electrostatic effect due to the counterion is needed to recover the correct absorption energy. The shielding effect that the protein dielectric exercises on E113 must not be full, as we need to recover only ca. 50% (i.e., ca. 7 kcal/mol) of the counterion blue shift; see Scheme 1. Remarkably, Table 2 shows that most of the residues responsible for this effect must be found nearby the retinal chromophore between the 2.5 and 3.5 Å shell, as it is from 2.5 to 3.5 Å that the counterion is mostly quenched and Rh absorption is recovered (see Scheme 1). Thus, these results reveal that only a limited number of actors (14 amino acids overall, see Table 2) are potentially involved in counterion quenching. To highlight the effect of these residues, an RFP analysis (see Computational Details) is performed on each of them and, for completeness, also on the Glu-113 counterion. The blue or red shift in the chromophore S_1 excitation energies with respect to the reference Rh value (that is represented by the zero line) is displayed in Figure 3 for each investigated residue.[65]

Very interestingly, Figure 3 shows that there is not a specific residue that is responsible alone for the 113 quenching, as this appears more as a cooperative effect of a rather limited number of polar residues surrounding the chromophore, namely Ser-186 (2.6), Thr-118 (1.6), Ala-117 (1.3), Hie-211 (1.0), Tyr-191 (0.7), and Tyr-43 (0.6) (the shielding effect in kcal/mol is reported in brackets); see Figure 3. These are the only residues (that are comprised between the 2.5 and 3.5 Å shell) that produce a significant backward red shift of the absorption maximum and *provide alone almost all the shielding power of the protein*. Figure 4 shows the position of these residues around the chromophore and the associated charges (in a colors code: from blue/negative to red/positive), and it provides a rationale for their effects. It is apparent that all the shielding residues display a significant positive (negative) charge close to the N-head (C-tail) of the chromophore that therefore produces a red shift in the absorption by destabilizing the ground state and stabilizing the excited state (the other way round occurs for blue shifting residues); see Scheme 2. Thus, the protein is designed here to produce a net effect that partially shields the primary Glu-113 counterion.

Fairly enough, it must be said that other surrounding polar groups (that are not comprised in the residues analyzed above) affect spectral properties, as they lead to a significant red/blue shift absorption as well. For instance, Glu-181, Glu-122, Tyr-192, Tyr-268, 292, 90, 261, 265, and 269 have been already recognized as important in dictating/affecting spectral tuning and optical properties. Specifically, Glu-181 and Glu-122 are charged/highly polar nearby amino acids; Tyr-192 and 268 are very close to the chromophore[29] and intervene in the H-bonded network;[66] amino acid change at site 292 in the C-terminus (transmembrane VII) causes a variable level of λ_{max}-absorption shift in different visual pigments[67] (it has been recently found that far distant amino acids are also able to modulate the absorption maximum of rhodopsins too);[68] sites 90, 261, 265, and 269 correspond to "key residues" for spectral tuning in color vision (i.e., cone pigments).[69,70] Although some of these residues produce a significant change in the absorption energy (see again Figure 3 for a RFP analysis of these groups), their net electrostatic effect is negligible: *it is only for the residues in the 2.5−3.5 Å shell that electrostatic effects add-up in a constructive manner, so that the primary counterion gets shielded*. This is the first time such an effect has been recognized, and experimentalists are now encouraged to target these residues in their studies (e.g., by mutation experiments) to prove and quantify their effects. More important, mutations involving residues that are crucial for spectral modulation and shielding efficiency could be responsible for vision pathologies related to Rh malfunctions, which is a further stimulus for experimental efforts in this direction. This issue will be discussed and studied in-depth in section 3.4 below.

In conclusion, we predict for Rh a situation of partial (ca. 50%) quenching of the 113 counterion, that falls between the two extreme scenarios presented by Buss/Morokuma/Nakatsuji[45,47,48] (no quenching, i.e., Rh absorbs as the ion-pair system) and Olivucci[31] (complete shielding, i.e., Rh absorbs as the distorted retinal in vacuo). This appears in line with recent QM/MM studies by Bravaya et al.[46] Interestingly, it is worth noting that we formally used the same approach as used by Buss[45] and Olivucci[31] (namely CASSCF(12,12)/CASPT2 energy calculations on the

(65) Notably, both reverse (Figure 3) and direct (Table 2) analyses do roughly agree for the E113 effect, the difference in the two results being due to the different polarization that the QM environment experiences in the two approaches: in the first we do have the full electrostatic environment of the protein but not the residue under investigation, while in the second we have only the electrostatic effects of the investigated residues.

(66) Yan, E. C. Y.; Ganim, Z.; Kazmi, M. A.; Chang, B. S. W.; Sakmar, T. P.; Mathies, R. A. *Biochemistry* **2004**, *43*, 10867.
(67) Fasick, J. I.; Lee, N.; Oprian, D. D. *Biochemistry* **1999**, *38*, 11593.
(68) Yoshitsugu, M.; Shibata, M.; Ikeda, D.; Furutani, Y.; Kandori, H. *Angew. Chem., Int. Ed.* **2008**, *47*, 3923.
(69) Lin, S. W.; Kochendoerfer, G. G.; Carroll, H. S.; Wang, D.; Mathies, R. A.; Sakmar, T. P. *J. Biol. Chem.* **1998**, *273*, 24583.
(70) Coto, P. B.; Strambi, A.; Ferre, N.; Olivucci, M. *Proc. Natl. Acad. Sci. U.S.A.* **2006**, *103*, 17154.

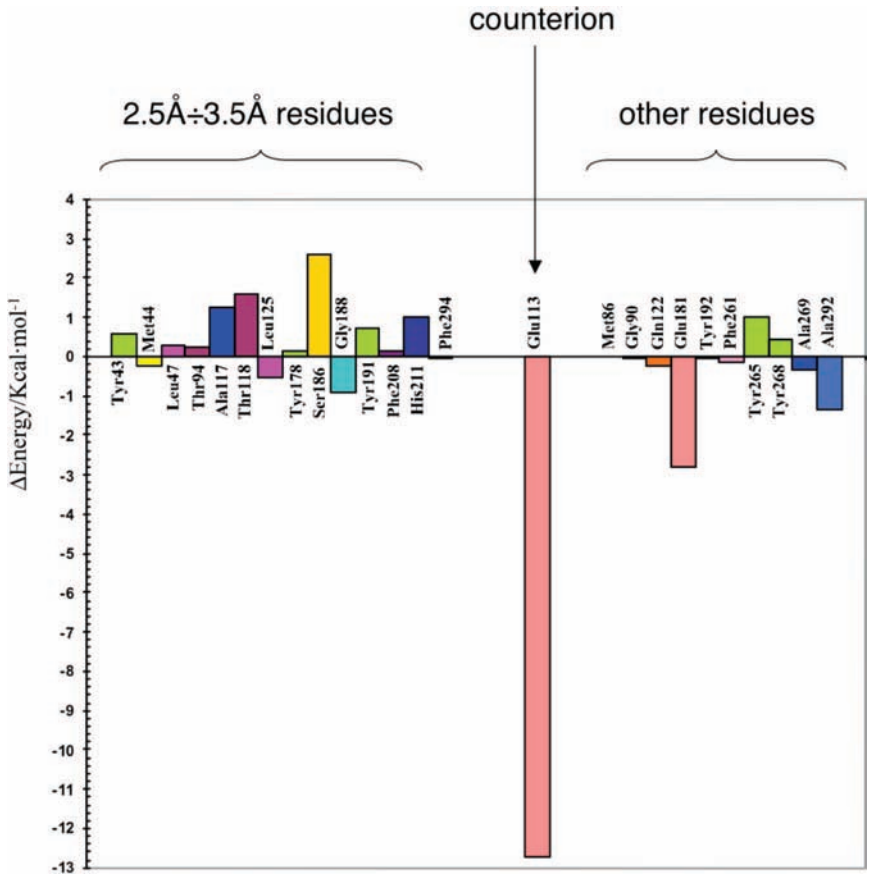

Figure 3. Reverse Fingerprint (RFP) analysis of the 14 rhodopsin residues comprised within a 2.5−3.5 Å radius around the chromophore, the counterion, and other residues recognized relevant for spectral tuning in the visual pigments. All the reported values refer to CASPT2 corrected energies.

chromophore put in the bath of the protein point charges). Anyway, Buss's calculations (leading to a negligible protein red-shift effect) are done on top of a chromophore structure optimized via a DFT-based method, while Olivucci's results and ours (both leading to a high red-shift effect that significantly compensates the counterion) are produced using a CASSCF optimized retinal (this was done to be as consistent and homogeneous as possible with respect to the CASPT2 approach employed for computing correlated energies and electronic transition properties). We are convinced this argument holds the key for the different computational outcomes, as DFT-based methods yield a chromophore structure with underestimated bond length alternation and overemphasized positive charge delocalization that is very different than the CASSCF one. This leads to a different response of the chromophore to the surrounding charges and the protein dielectric in general that may account (at least partially) for the observed discrepancies.

3.2.2. Photoreactivity Effects. Tuning the Slope of the Photoisomerization Channel. The counterion dependent destabilization of the S_1 energy that has been recognized at the FC point is foreseen all along the points of the S_1 path. Moreover, we expect this effect not to be identical but to increase steadily along the path as the charge transfer character of the S_1 (B_u-like) state is increasing upon rotation,[15] reaching a maximum at the twisted funnel point where a net charge transfer occurs (see bar diagrams in Figure 2): this is the point where external electrostatic effects on the S_1 energy are expected to be the highest. Thus, it is apparent that the electrostatic effects can also play a role in the photoisomerization process, as the slope of the channel and the location/existence of the twisted conical intersection funnel and crossing seam can change. To quantify these effects the energy of the MEP computed in Rh has been reevaluated in two different electrostatic conditions, i.e., into a protein environment where all external charges have been switched off ($Rh_{no\text{-}charges}$) and where only the counterion charge has been explicitly considered (Rh_{113}). So doing, all protein steric constraints have been preserved, although electrostatic effects have been zeroed ($Rh_{no\text{-}charges}$) or limited only to Glu-113 (Rh_{113}), respectively. Thus, while the former reproduces the scenario for a fully quenched counterion, the latter displays the limiting situation of a fully unquenched counterion.

Figure 5 summarizes these results by comparing the path and key points calculated for $Rh_{no\text{-}charges}$ (see Figure 5a), Rh (see Figure 5b), and Rh_{113} (see Figure 5c), while Table 3 reports the corresponding energies. The shielding effect that the protein dielectric exercises on the counterion (that results into a red shift in the S_1 energy with respect to the ion pair) weights ca. 7 kcal/mol at the FC point that, as shown in the previous section, is ca. 50% of the overall counterion blue-shift effect at FC (that ranges from 14.4 to 15.4 kcal/mol depending on the calculation level adopted; see Scheme 1 and Figure 5c). On the other hand, the overall counterion blue-shift effect is estimated to be ca. 34 kcal/mol at the twisted structure (see Table 3 and Figure 5c). Notably, this is roughly twice the value calculated at the FC point as we have a net (half) charge transfer at the CI (FC). As anticipated above, this is the trend expected for S_1: counterion destabilization on S_1 energies increases upon increasing the charge transfer character of S_1, i.e., upon rotation. Calculations show (see Table 3 and Figure 5b and 5c) that counterion shielding in Rh recovers ca. 23 kcal/mol at the CI_{Rh}.

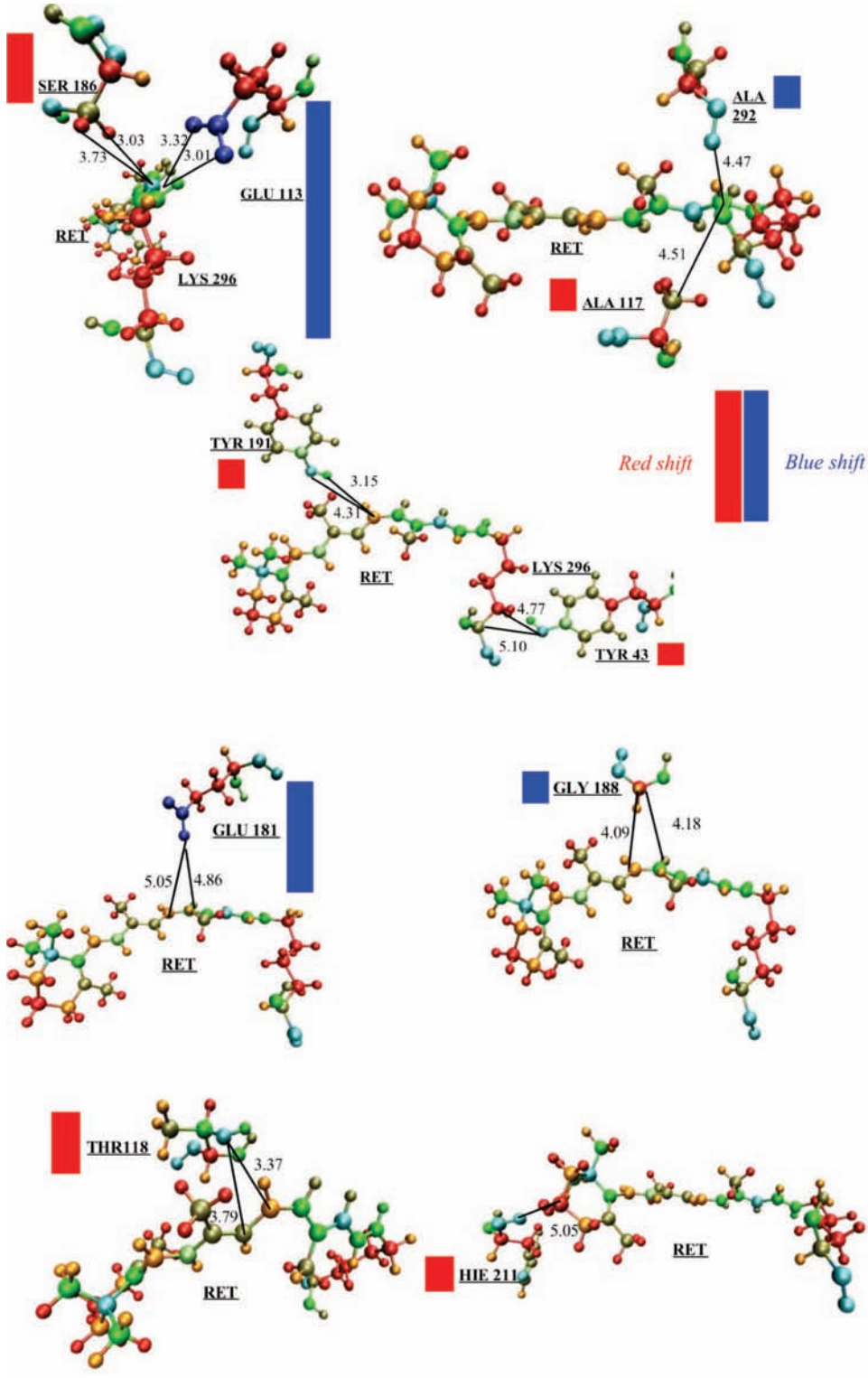

Figure 4. Displacement around the chromophore of the residues mostly relevant for counterion shielding and corresponding charges analysis. The color spectrum from blue to red displays negative to positive partial charges on the atoms, respectively. Bar blue/red diagrams display the blue/red shift effect for each residue as shown also in Figure 3.

Another consequence of these effects is that the slope of the photoisomerization channel becomes dramatically decreased in Rh_{113} (as it increases the destabilization of the counterion along the path; see Figure 5c). Eventually, a barrier emerges along the path and an excited-state intermediate appears (M^{ion}_{113}) preventing an efficient twisting. More interesting, the CI funnel disappears and a twisted point (TP_{113}) with a large S_1/S_0 energy gap separation (ca. 21 kcal/mol; see Figure 5c) replaces it. Thus, it is apparent that the crossing seam has been removed (or displaced to much higher energies that are not of (photo)chemical relevance). To further investigate this issue and unambiguously define this mechanistic picture, we have fully optimized (into the protein and in the field of the counterion charges alone, i.e., Rh_{113}) both the excited-state intermediate (M^{ion}_{113}) and the

Scheme 2. Blue/Red Shift Effect on the Absorption of the Chromophore Due to the Nearby Dipoles of the Residues[a]

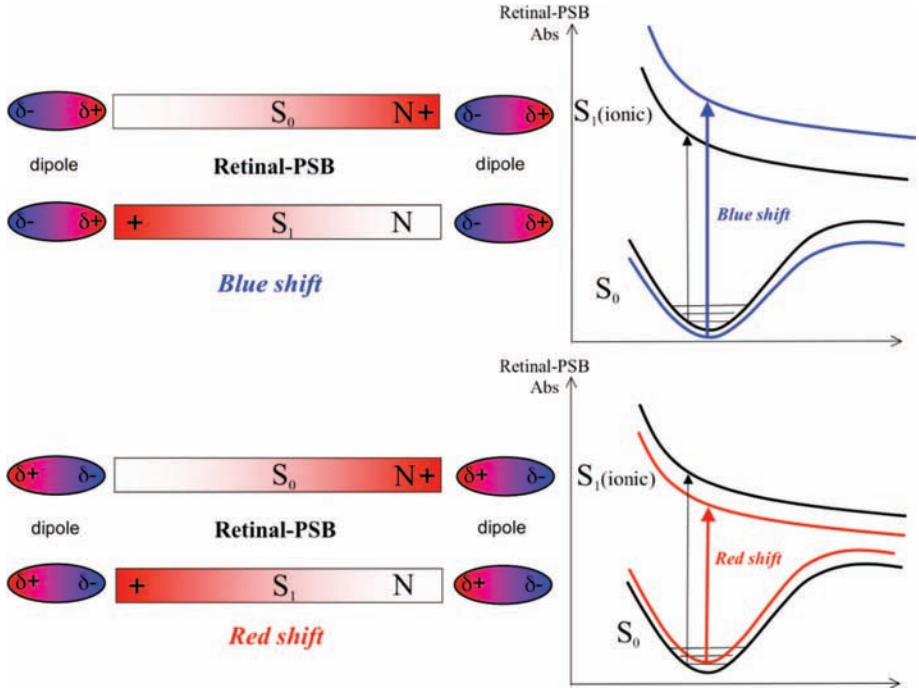

[a] Positive/negative charges are displayed in red/blue, while the linear polyenic chain of the chromophore is represented as a horizontal bar.

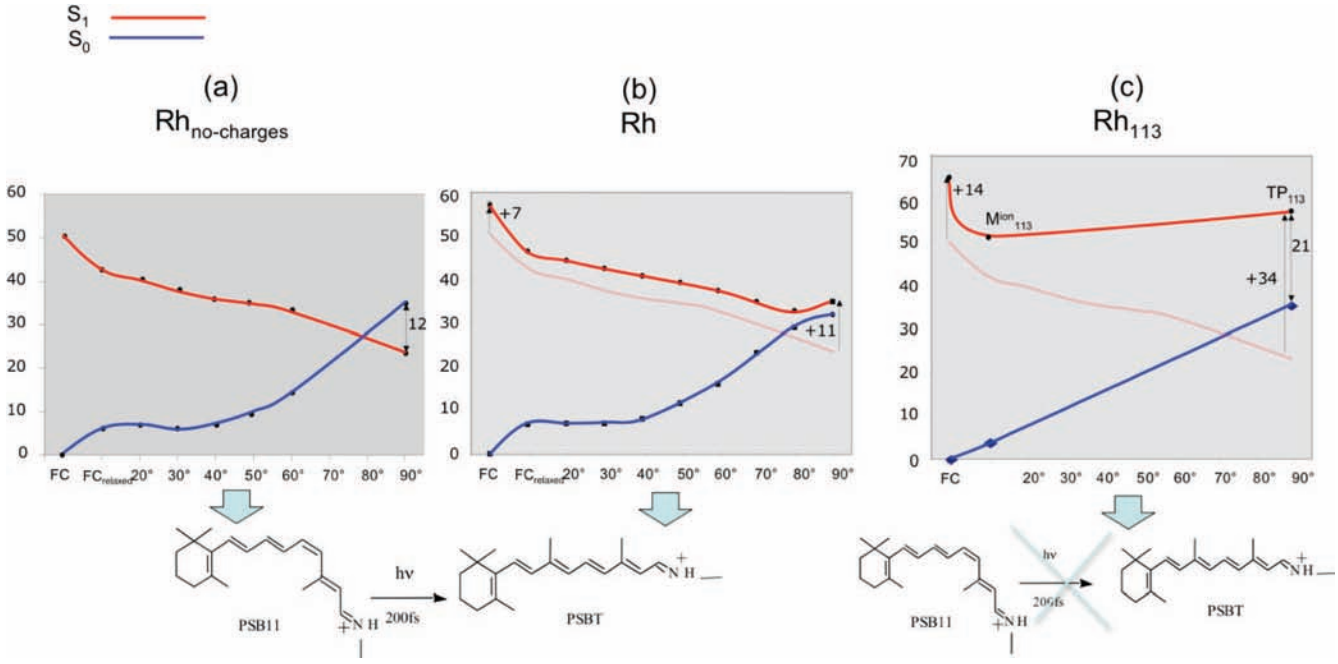

Figure 5. The S_1 and S_0 energy profiles (kcal/mol) along the S_1 photoisomerization MEP computed in Rh (b) have been reevaluated in the protein without charges (a) or only with the counterion charge (c). The profile displayed in (a) is also reported as a shaded line in (b) and (c). CASPT2 energies are reported in (a) and (b), while MS-CASPT2 values are reported in (c).

twisted structure of the chromophore (TP_{113}). These results (that are shown in the Supporting Information) confirm the mechanistic picture shown in Figure 5c. It is apparent that the 21 kcal/mol S_1/S_0 energy gap found at TP_{113} prevents any efficient (and ultrafast) internal conversion process in Rh_{113}. Interestingly, this energy gap is the *minimum* energy that the protein dielectric must recover (by shielding the counterion) to generate a conical intersection funnel and trigger an efficient (i.e., ultrafast) photoisomerization process. Although this quenching does not appear full, it is significant and is estimated to be ca. 60% (i.e., 21 kcal/mol) of the overall counterion blue-shift effect at the twisted structure (i.e., 34 kcal/mol): *this is the least shielding that we need to have photoactive visual pigments*. Remarkably, this is almost identical to the shielding that is estimated in Rh at the twisted point (23 kcal/mol) and that is needed to recover S_1/S_0 degeneration and generate a twisted conical intersection.

It can be concluded that *the quenching of the counterion by the protein (by at least a 60% shielding factor in the twisted*

Table 3. CASPT2 Relative Energies (ΔE, kcal/mol) for the Lowest Three Singlet States, Oscillator Strengths for Ground State Excitations ($f_{S_0 \rightarrow S_n}$) and Wavefunction Characterization at the Franck−Condon (FC) and Twisted Structures of the Rhodopsin Photoisomerization Path Computed in the Protein with Three Different Electrostatic Environments: No Charges ($Rh_{no\text{-}charges}$), All Charges (Rh), Only the Counterion Charge (Rh_{113})

environment	structure	chromophore state (electronic nature)	ΔE	$f_{S_0 \rightarrow S_n}$	wave function[a]
$Rh_{no\text{-}charges}$	FC point	S_0	0.0	0.00	$(6a)^2$ $(7a)^0$ (0.78)
		S_1	50.3	0.78	$(6a)^1$ $(7a)^1$ (0.65)
		S_2	79.3	0.23	$(6a)^0$ $(7a)^2$ (0.15)
					$(6a)^1$ $(7a)^1$ (0.13)
	twisted stucture (twisted PSB11 found in CI_{Rh})	S_0	23.1	0.00	$(6a)^2$ $(7a)^0$ (0.81)
		S_1	35.1	0.003562	$(6a)^1$ $(7a)^1$ (0.74)
		S_2	86.9	0.000623	$(6a)^1$ $(8a)^1$ (0.30)
					$(5a)^1$ $(6a)^1$ $(8a)^2$ (0.74)
Rh	FC point	S_0	0.0	0.00	$(6a)^2$ $(7a)^0$ (0.77)
		S_1	57.6	0.74	$(6a)^1$ $(7a)^1$ (0.63)
		S_2	82.0	0.27	$(6a)^0$ $(7a)^2$ (0.11)
					$(6a)^1$ $(7a)^1$ (0.19)
	twisted stucture (CI_{Rh})	S_0	32.5	0.00	$(6a)^1$ $(7a)^1$ (0.73)
		S_1	34.5	0.00001316	$(6a)^2$ $(7a)^0$ (0.82)
		S_2	84.8	0.00000875	$(6a)^1$ $(8a)^1$ (0.31)
					$(5a)^1$ $(6a)^1$ (0.34)
Rh_{113}	FC point	S_0	0.0[b] (0.0)	0.0	$(6a)^2$ $(7a)^0$ (0.75)
		S_1	65.7[b] (75.7)	0.13566	$(6a)^1$ $(7a)^1$ (0.54)
		S_2	95.2[b] (74.7)	0.74604	$(6a)^0$ $(7a)^2$ (0.23)
					$(6a)^1$ $(7a)^1$ (0.18)
	twisted stucture (TP_{113})	S_0	35.7[b] (32.6)	0.000127	$(6a)^1$ $(7a)^1$ (0.70)
		S_1	59.8[b] (57.1)	0.000578	$(6a)^2$ $(7a)^0$ (0.79)
		S_2	88.3[b] (84.7)	0.03199	$(5a)^1$ $(6a)^1(7a)^2$
					(0.33) $(6a)^1$ $(8a)^1$ (0.12)
					$(6a)^1$ $(9a)^1$ (0.15)
	M^{ion}_{113}	S_0	4.3[b]	0.00	$(6a)^2$ $(7a)^0$ (0.64)
		S_1	51.2[b]	0.7182	$(6a)^1$ $(7a)^1$ (0.53)
		S_2	78.4[b]	0.006818	$(6a)^0$ $(7a)^2$ (0.21)
					$(6a)^1$ $(7a)^1$ (0.14)

[a] 6a and 7a represent the delocalized HOMO and LUMO π molecular orbitals at the FC point, respectively. At the twisted structure π orbitals localize on each semifragment, with 6a that is localized on the N containing half and 7a that is localized on the β-ionone containing half. Consequently, at the twisted structure the closed shell $(6a)^2$ $(7a)^0$ configuration describes the charge transfer state (that is diabatically connected to $S_1/(6a)^1$ $(7a)^1$ in the FC point), while the open shell $(6a)^1$ $(7a)^1$ configuration describes a diradical state (that is diabatically connected to $S_0/(6a)^2$ $(7a)^0$ in the FC point). [b] Multistate CASPT2 results: corresponding CASPT2 values are in brackets, when reported.

structure) is a prerequisite to have an efficient and ultrafast photoisomerization in visual pigments: it recovers a barrierless path and a twisted CI funnel. Thus, besides providing a tool for spectral tuning that regulates absorption energies, counterion quenching is also mechanistically fundamental since it promotes photoisomerization catalysis that would be otherwise depressed if the counterion were unshielded.

Interestingly, a consequence of the above reasoning is that if we produced a mutated Rh with an altered (i.e., smaller) counterion shielding power, the photoreactivity of the pigment would be impaired and fluorescence (e.g., from the M^{ion}_{113} intermediate) may become a competitive process. Experimental investigations in this direction (by site directed mutations of those residues recognized here as responsible of the shielding efficiency such as Ser-186, Thr-118, Ala-117, Hie-211, Tyr-191, Tyr-43, Tyr-265) would be welcome as this would provide the way to switch from a photoisomerizable to a fluorescent device.

3.3. Spectral Tuning Mechanism in Color Vision. Several factors have been recognized (alone or concurrently) as possible candidates for color tuning in visual pigments: retinal twist, protein electrostatic field, interaction with the counterion (i.e., H-bonding and charge transfer), and protein polarization (different number of aromatic residues near the chromophore). Notably, the 435 to 570 nm range of S_1 excitation wavelengths spanned by the vacuo($PSB11_{dist}$)/ion-pair($PSB11_{dist}$−113E) systems covers the appropriate range for the color pigments S (425nm), M (530 nm), and L (560 nm); see Scheme 1. This suggests the working hypothesis that such a spectral modulation could be achieved in principle by tuning the shielding effect of the 113 counterion from a fully quenched (vacuo-like) system (that reproduces the red absorption of the L-cone pigment) to the unquenched ion pair (that absorbs in the blue as the S-cone pigment), through an intermediate state absorbing in the green (M-cone pigment) where the counterion is only partially quenched. As a result, a tunable shielding of the counterion could appear as a suitable tool for regulating color absorptions. In light of the mechanistic results presented above, it is apparent that *the absorption of the blue (S-cone) pigment cannot be achieved by a fully unquenched 113 residue*: this would produce the correct blue absorption found in the ion pair, but it would lead to an inefficient photoreaction. In fact, we have proved that the counterion must be significantly shielded to have a photoactive pigment: at least a 60% shielding factor must be operative at the twisted structure. This means that also other mechanisms must cooperate to recover the ca. 10 kcal/mol needed to reach the high absorption energy of the blue pigment (from 57 kcal/mol in Rh to 67 kcal/mol in S), as the counterion

shielding cannot be further reduced. We have suggested in previous works[71] that the β-ionone handle may be also used as a regulatory tool for absorption energies. In fact, a fully twisted β-ionone ring should produce a blue-shifted retinal absorption, as the chromophore conjugation has been reduced. Interestingly, recent experimental investigations on a Rh with an acyclic retinal analogue (i.e., lacking the β-ionone ring) show that this absorbs at 460 nm,[72] corresponding to a ca. 5 kcal/mol blue shift of the Rh wild-type absorption. This is also the shift that is expected in a chromophore with a fully deconjugated β-ionone ring. Anyway, this is only half the energy that we need to recover S-pigment absorption. Thus, it is apparent that this effect alone is not sufficient and that a further deconjugation of the chromophore (triggered by steric interactions with the protein pocket) is necessary. That is achieved for example by twisting about one (or more) of its internal double bonds (such as the C_8-C_9 single bond), thus leading to a higher energy absorbing chromophore. Remarkably, recent experimental works on a Rh-containing retinal analogue with only four conjugated double bonds (i.e., a 7,8-dihydro retinal has been used)[73] show that this chromophore already absorbs at blue energies (435 nm), as found in the S-cone pigment and, more importantly, preserves the photoisomerization ability and the photoacitivity of the blue-cone analogue so far obtained. Thus, if the protein binding pocket of this pigment is designed to force the retinal chromophore into a conformation with a highly distorted structure (e.g., fully twisted about the C_8-C_9 single bond), a blue absorption should be already observed without the need for other effects. On the other hand, a complete (partial) shielding of the counterion by the protein dielectric appears as the most viable way to produce alone the lower energy absorbing L (M) pigment: this would preserve the photoactivity of the pigment itself as counterion shielding would be higher than 60%. Scheme 1 summarizes these results.

Interestingly, this reasoning agrees with the similarity in the structure of the L and M opsins (they share over 96% amino acid sequence identity and their higher homology correlates with the smaller absorption shift and has evolutionary reasons) and the different structure observed in the S pigment (only 43% identity with L and M),[74,75] as here the binding pocket must be differently designed so that a highly twisted chromophore is hosted (which causes the very different sequence identity). Additionally, this spectral tuning mechanism validates the tentative structures for the L, M, and S pigments that have been very recently generated using homology modeling techniques:[76] while the chromophore structure appears very similar in both the L and M pigments, its conformational twisting plays a major role in the S-pigment, as retinal appears much more distorted in this environment, interestingly due to one exchange amino acid relative to L/M. On the other hand, dipolar side chains are shown to play a large role in the opsin shift from red to green. A detailed analysis of the color tuning mechanism has been also reported very recently by Fujimoto et al.[77]

Finally, it must be pointed out that the above reasoning is far from being conclusive and experimentally proven, as a univocally accepted mechanism is not yet available for cone pigment spectral tuning and contradictory results (both experimental and computational) exist: the last words on this issue will not probably be written until resolved structures for the color-cone pigments (and the blue-cone in particular) become available. Experimental evidence exists that has been used to support a contrasting, pure electrostatically driven, spectral tuning mechanism. Reference 20 shows that nine concurrent point mutations exist that turn Rhodopsin into a blue-cone analogue mutant chimera. Those mutations seem to produce an electrostatic effect only, as retinal does not appear to be locally perturbed and its structure seems preserved according to resonance Raman vibrational spectra. It is also true that the blue-cone analogue photoactivity is disrupted; i.e., it is not able to activate transducin anymore. Why this occurs is not yet clear: isomerization seems to occur, but no clear statement on this point can be made based on the available spectroscopic evidence, and in any case no data are available for both the photoisomerization QY and its rate that can be both highly affected by those mutations (the only clear thing is that formation of meta-II species is prevented). Thus, all these issues are still largely elusive. On the other hand, recorded vibrational features (HOOP modes) that are unchanged in the different cone pigments are taken as a clue for a similar and unchanged chromophore structure. Although vibrational signatures are of great help in elucidating the structures of the targeted molecule, also great care and caution must be used in interpreting these results, as these features may turn out to be quite elusive in revealing the exact conformation of the chromophore, in particular when the structural difference is located about a C−C single bond that is quite far from the vibration center (e.g., twisting about the C_8-C_9 single bond, as suggested here, vs the $C_{11}H-C_{12}H$ HOOP). A clear example of that is provided by the still debated structure of the phytochrome chromophore: a *ZZZasa* structure is assumed on the basis of vibrational spectroscopic arguments, but this is still widely under discussion, as good spectroscopic arguments for this and the other conformation of the C4−C5 bond (*ZZZssa*) have been presented. This situation resembles the one discussed in the paper for the protonation state of the 181 residue: while spectroscopic data for E181 point mutations have been previously used to define its neutral state,[37,38] it has been recently pointed out[39] (and this has been deeply discussed in this paper: see section 3.1) that absorbance measurements on those Rh mutants are not suitable to assess whether E181 is ionized in the dark, as this residue is placed right above the central $C_{11}=C_{12}$ double bond of retinal (i.e., in a symmetric position with respect to the PSB head and the β-ionone tail of the chromohore), which makes S_1 rather insensitive to its protonation state. This example tells us how previously solid conclusions based on experimental evidence have been reconsidered in light of new understandings.

In conclusion, we think that a final statement cannot yet be drawn, as some works point to a pure electrostatic tuning while others to a different (e.g., retinal twist) contributor, as in our paper. A blend of them may be likely involved, although our results clearly reveal that a pure (unquenched) counterion effect

(71) Cembran, A.; González-Luque, R.; Altoè, P.; Merchán, M.; Bernardi, F.; Olivucci, M.; Garavelli, M. *J. Phys. Chem. A* **2005**, *109*, 6597.
(72) Bartl, F. J.; Fritze, O.; Ritter, E.; Herrmann, R.; Kuksa, V.; Palczewski, K.; Hofmann, K. P.; Ernst, O. P. *J. Biol. Chem.* **2005**, *280*, 34259.
(73) DeGrip, W. J.; Bovee-Geurts, P. H. M.; van der Hoef, I.; Lugtenburg, J. *J. Am. Chem. Soc.* **2007**, *129*, 13265.
(74) Nathans, J.; Thomas, D.; Hogness, D. S. *Science* **1986**, *232*, 193.
(75) Neitz, M.; Neitz, J. Color Vision Defects. *Encyclopedia of Life Sciences*; John Wiley & Sons, Ltd: 2005.
(76) Trabanino, R. J.; Vaidehi, N.; Goddard, W. A. *J. Phys. Chem. B* **2006**, *110*, 17230.
(77) Fujimoto, K.; Hasegawa, J.; Nakatsuji, H. *Chem. Phys. Lett.* **2008**, *462*, 318.

would impair the retinal photoisomerization efficiency and, ultimately, the pigment photoactivity. Under this point of view, we think that cooperation of a conformational effect must be operative.

3.4. Mutations and Vision Deficiencies. 3.4.1. Rh Related Vision Deficiencies. It has been shown above that several Rh residues appear as major players in spectral modulation (by a regulatory mechanism of the shielding effect) and their effect has been quantified in Table 2 and Figure 3. It is likely that natural mutations involving those groups may compromise more than others the optical properties and photoactivity of the photoreceptor and may be the source of vision pathologies related to Rh malfunctions. More specifically, we suggest here that *many of the mutations impairing the photoactivity of Rh do that by reducing its counterion shielding efficiency*: indeed we have seen that at least a 60% shielding power must be operative at the twisted structure to preserve the photoefficiency of the pigment. If it is reduced below that threshold, an inefficient photoisomerization that impairs Rh photoactivity should result.

Over one hundred mutations have been recognized until now to cause retinitis pigmentosa 4 (in the genetic classification of retinitis pigmentosa, the form that is due to mutations in the rhodopsin gene is referred to as retinitis pigmentosa 4).[78,79] If we exclude those mutations that inactivate Rh by disrupting its structure and stability (or that of its photocycle intermediates) or its ability to bind G-protein, it is conceivable that the remaining ones harm Rh because they prejudice its counterion shielding power (i.e., counterion shielding gets below the 60% threshold value). Thus, as long as we deal with electrostatic effects only, we could suggest that counterion-shielding groups are the best candidates for a replacement that impairs the photoactivity efficiency of the pigment and thus render the protein inactive; additionally, this inactivating effect is expected to be as big is the deshielding power of the replacing group, thus amplifying the effect of the missense (i.e., single point) mutation. Although, as said above, effects other than the electrostatic one may likely participate to inactivate the pigment (e.g., structural effects), it is interesting to note that, of the many mutations recognized to cause retinitis pigmentosa 4, some involve the counterion-shielding groups investigated here such as, among others, Ser-186 and His-211 that are the ones with the highest shielding power (see Figure 3).

It must be pointed out that the suggestion we are putting forward is far from being conclusive and experimentally proven and is based on the assumption that our computational model is quantitatively correct. A systematic computational analysis of those genetic changes is out of the scope of this work and would be welcome, as well as new experimental investigations. Yet, the collected data on Rh make this hypothesis computationally sound. To the best of our knowledge, this is a new paradigm in Rh-related vision pathologies that experimentalists are now encouraged to investigate and address (e.g., by novel mutation experiments). If positive, these experimental proofs would provide a validation of the above model as well as open a new scenario in the rationale of eye diseases.

3.4.2. Color Pigments Related Pathologies. It is worth noting that mutations related to color blindness in humans are known to be mostly located in the red (L) and green (M) cone pigments, while the blue (S) pigment is much less effected.[75] We suggest this is also a clue for a different color tuning mechanism in the former pigments with respect to the latter, which is based on a tunable counterion quenching and chromophore conformational control, respectively (as shown in section 3.3 and Scheme 1 above). The first is by definition very sensitive to changes in the electrostatic environment (such as the ones due to mutations) that could alter the optical response of the pigment and can involve potentially all the surrounding polar residues that are found to be important in spectral tuning. We have seen here (see Figure 3) that many residues may play such a role in Rh and all appear as good candidates for mutations leading to color vision deficiencies: less than 3 kcal/mol separates the absorption energy of the L and M pigments, and most of these residues produce spectral modulations falling in the 1−3 kcal/mol range. On the other hand, a much larger energy gap (ca. 13 kcal/mol) separates the green (M) from the blue (S) pigment absorptions, and once the retinal is accommodated into the protein pocket, it is much harder for a missense mutation to alter its optical properties and photoactivity efficiency so strongly, as these are mostly regulated by the steric dependent conformational twisting of the chromophore. It is worth stressing here that this reasoning focuses on those residues and mutations that are involved in spectral tuning only, while it neglects all those genetic changes that inactivate the photopigment by disrupting its structure or stability (which may be another source of vision deficiency).

4. Conclusions

We have provided computational evidence that electrostatic effects do strongly control both spectral and photoreactivity properties in visual pigments and that the two concepts are strictly related to each other: a unified model has been produced that discloses the key role played by counterion quenching in assisting retinal photoisomerization and setting up its optical features. Based on that, a sound mechanism for spectral tuning in color vision pigments emerges. Although this appears in disagreement with previously reported interpretations and is yet far from being conclusive, we show that it is also validated by recent experimental and molecular dynamics investigations and provides a rationale for the different structures found in the M/L pigments as compared to the S one. These results suggest a new paradigm in vision deficiencies related to Rh mutations, as night blindness may also result by an impaired counterion shielding efficiency in the mutated pigment. It is also shown that the ease in M/L malfunctions with respect to the ones found in S can be easily accounted for by considering the different mechanism for color modulation found in those pigments.

In conclusion, these results contribute to the understanding of the factors controlling spectral modulation and photoisomerization catalysis in rhodopsins and suggest that vision pathologies may be also produced by mutations that harm the counterion shielding power of the visual pigment. To the best of our knowledge, this is a novel concept in vision deficiencies that experimentalists are now encouraged to investigate and address. Finally, it has been pointed out that an intriguing consequence of the presented results is that it would be possible in principle to design modified (i.e., mutated) rhodopsins with a smaller counterion shielding power that can become fluorescent. That is, playing with the protein electrostatic field would be the way

(78) McKusick, V. A. et al. RHODOPSIN; RHO. In *OMIM: Online Mendelian Inheritance in Man*; Johns Hopkins University:http://www.ncbi.nlm.nih.gov/entrez/dispomim.cgi?id=180380.
(79) Okada, T.; Ernst, O. P.; Palczewski, K.; Hofmann, K. P. *Trends Biochem. Sci.* **2001**, *26*, 318.

to switch from photoisomerizable devices to fluorescent dyes, and the rationale for such a molecular design has been provided here.

Acknowledgment. The research reported has been supported by funds for Selected Research Topics, MURST PRIN 2005 (project: "Trasferimenti di energia e di carica a livello molecolare"), FIRB (RBAU01L2HT) and Spanish MEC-FEDER CTQ2007-61260 and CSD2007-0010 Consolider-Ingenio in Molecular Nanoscience projects. GOG gratefully acknowledge Ph.D. fellowships from the Spanish MEC. E4 Computer Engineering Spa is gratefully acknowledged for granted computational time and technical assistance.

Supporting Information Available: Details of the QM/MM scheme adopted in this work (section S1 and Figure S1), validation of MS-CASPT2 results (section S2, Tables S1−S7 and Figure S2), complete refs 51 and 55 (section S3), energies and coordinates of all the structures discussed in the paper (section S4). This material is available free of charge via the Internet at http://pubs.acs.org.

JA808424B